STEREOSCOPIC CLOUD BASE RECONSTRUCTION USING HIGH-RESOLUTION WHOLE SKY IMAGERS

Florian M. Savoy,[1] *Soumyabrata Dev,*[2] *Yee Hui Lee,*[2] *Stefan Winkler*[1]

[1] Advanced Digital Sciences Center (ADSC), University of Illinois at Urbana-Champaign, Singapore
[2] School of Electrical and Electronic Engineering, Nanyang Technological University (NTU), Singapore

ABSTRACT

Cloud base height and volume estimation is needed in meteorology and other applications. We have deployed a pair of custom-designed Whole Sky Imagers, which capture stereo pictures of the sky at regular intervals. Using these images, we propose a method to create rough 3D models of the base of clouds, using feature point detection, matching, and triangulation. The novelty of our method lies in the fact that it locates the cloud base in all three dimensions, instead of only estimating cloud base height. For validation, we compare the results with measurements from weather radar.

***Index Terms*—** Ground-based sky camera, WAHRSIS, cloud base height, stereo reconstruction

1. INTRODUCTION

Ground-based localized cloud monitoring using Whole Sky Imagers is becoming common nowadays [1]. Precise information about the position of clouds in the atmosphere is needed for several applications. In solar energy, the power output of solar panels depends on the amount of solar radiation reaching them. Monitoring clouds and how they affect the sun light is thus needed for forecasting energy production [2]. In meteorology, cloud base height and volume are required for accurate monitoring and forecasting of the weather. Furthermore, information about cloud formations along the signal path of air-to-ground and air-to-air communications [3] helps quantify the attenuation due to clouds and rain. All these applications require a precise estimate of the localization of clouds at a resolution which is not achievable by satellite imaging.

We built our own Whole Sky Imagers (WSIs), which we call WAHRSIS (Wide Angle High Resolution Sky Imaging System) [4,5]. Each WAHRSIS is composed of an 18-MPixel DSLR camera with a fish-eye lens, enclosed in a box with a transparent dome. A single-board-computer controls the camera and sends the captured pictures to a server. We combine multiple pictures captured in quick succession with different exposure times into High Dynamic Range (HDR) images.

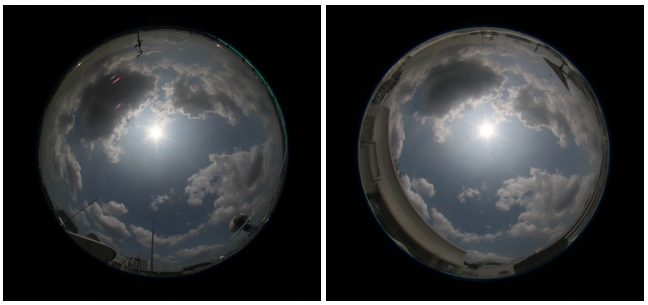

Fig. 1: Sample images captured simultaneously by our pair of sky imagers.

With an accurate localization of the imagers and calibration of the devices, a 3D model of the base of the clouds is constructed by triangulation. We use several undistorted images at various inclination angles from two fish-eye input images taken at the same time. The resolution and the increased contrast of HDR images allows us to perform dense feature point detection and matching, which are then used for triangulation. We finally compute wire-frames representing individual clouds from the reconstructed points.

This setup is very different from a traditional stereoscopic 3D reconstruction of a scene. The baseline is large (about 100 meters), and cameras can only be deployed on the ground, limiting the range of viewpoints available. These restrictions make calibration much more challenging than in a traditional stereo setup, since both cameras are not physically mounted on a common structure. We have devised a method which uses the location of the sun throughout the day to measure and model the misalignment [6]. The imagers needs to be synchronized in order to capture frames at the same time. Furthermore, multi-view stereo methods such as visual hulls or space carving are inappropriate [7]. Clouds often exhibit no sharp features or clear borders, and only sparse reconstruction methods prove to be suitable.

The problem of cloud reconstruction has been studied before. Allmen and Kegelmeyer [8] use Whole Sky Imagers developed at the Scripps Institution of Oceanography [9] to

This research is funded by the Defence Science and Technology Agency (DSTA), Singapore.

Send correspondence to stefan.winkler@adsc.com.sg

compute cloud base height. They apply epipolar geometry as well as pixel values and optical flows to match points from both imagers before triangulation, with a pseudo-Cartesian transformation to remove the fish-eye undistortion effect. Seiz et al. [10] use Förster and Harris detectors to extract features and map them with least-squares matching and a hierarchical pyramid-based approach. Kassianov et al. [11] use the size of the overlapping area between two images captured with a field of view of 100 degrees. However, all these prior works use images with a significantly lower resolution than the ones captured by our imagers. Fine details in the cloud texture are thus not captured and cannot be used as features.

Janeiro et al. [12] use two DSLR cameras to compute cloud base height as well as wind speed and wind direction. The calibration is done using stars and an affine transformation. They use normalized cross-correlation to map images, estimating the altitude of each layer. In an earlier proof-of-concept study with computer-generated images, we used scene flow to recover cloud base height [13].

The novelty of our method resides in the reconstruction of a dense point cloud, where every feature point is assigned a different 3D coordinate. Unlike previous methods, ours reproduces the shape of the bottom of clouds. By carefully geo-referencing our stereo setup and incorporating cloud/sky segmentation into the process, we are able to not only derive cloud base height, but also locate clouds in 3D real world coordinates. This is needed to study the effects of clouds along the light path between the sun and a solar panel or along the signal path in atmospheric communications. It is a first step towards short-term forecasting of 3D cloud movements.

2. TECHNIQUE

Our technique is based on matching feature points from several undistorted versions of the input images. This section first details the undistortion procedure, the creation of the pairs of matches, the triangulation, and finally the grouping of points belonging to the same cloud.[1]

We use pairs of images taken by two of our Whole Sky Imagers [5], placed 100m apart on the rooftops of two buildings of the Nanyang Technological University in Singapore. Figure 1 shows an example of a pair of captured images.

2.1. Undistortion

The first step consists of removing the distortion due to the fish-eye lens. We use a ray-tracing approach, which we presented earlier in [13]. It is illustrated in Fig. 2. The original fish-eye image from Fig. 1(a) is shown in the imaging plane at the bottom. The hemisphere shows the projection of the color values of each incident light ray. At the top is the undistorted image, with each pixel being computed as the value of each light ray going through the pixel at its location, as illustrated for the corners of the image.

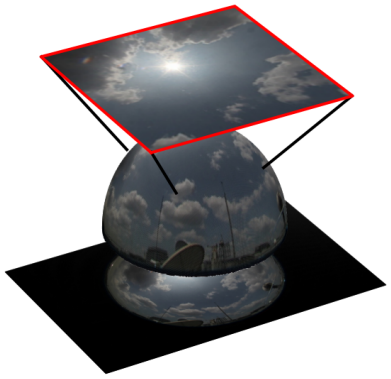

Fig. 2: Illustration of the picture undistortion process.

In order to map the undistorted images to real world coordinates, we define the undistorted image as a square of a side length of 1000 meters centered on top of the hemisphere at a height of 500 meters. By setting a pixel to have a size of one meter square, we obtain images of 1000×1000 pixels. This translates to a viewing angle of 90 degrees. We apply different rotations to this square to capture the clouds at the sides, as illustrated in Fig. 3. We use one horizontal square centered above the image center and 4 squares at an elevation angle of 35 degrees and azimuth angles of 0, 90, 180 and 270 degrees.

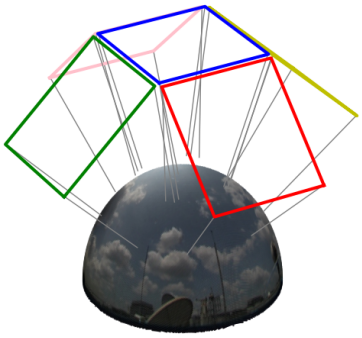

Fig. 3: Illustration of the different squares used in the undistortion process.

Furthermore, we transform the coordinates by the rotation matrix obtained through the calibration procedure described in [6] to cope with device misalignments. This method uses the sun trajectory across the frames captured throughout an entire day. It detects the sun in the images and uses the respective sun positions computed by astronomical equations [14] to quantify the misalignment of the imagers. With an accurate localization of the devices, it also geo-references the reconstructed models. The result of undistorting the input image shown in Fig. 1 can be seen at the top of Fig. 2.

[1] The source code of our method is available at: https://github.com/FSavoy/cloud-base-reconstruction

2.2. Feature Points Matching and Triangulation

Our Whole Sky Imagers capture HDR images by taking three successive images with varying exposure times. We use tone-mapped images created by the algorithm described in [15] as input to the feature points matching algorithm.

We use the OpenCV implementation of SIFT feature points detection and matching to compute feature points, along with a brute force matching and Lowe's ratio test [16]. We apply it on each pair of undistorted squares independently of each other. Figure 4 shows an example of matching features between the various pairs of undistorted images.

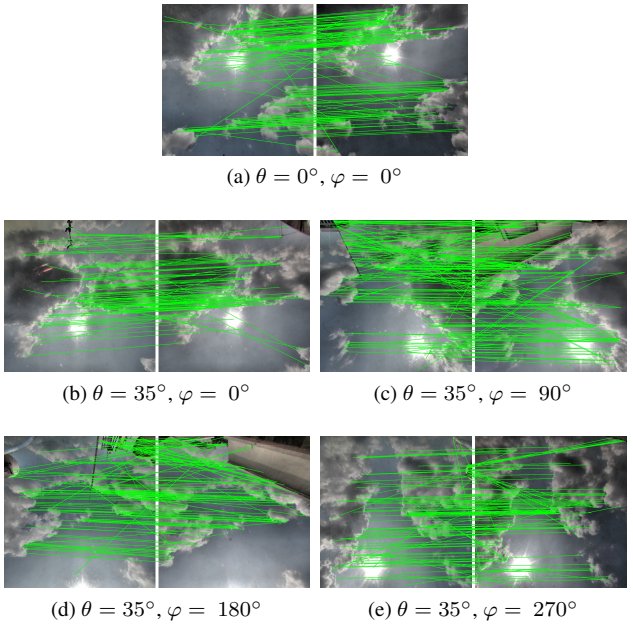

(a) $\theta = 0°, \varphi = 0°$

(b) $\theta = 35°, \varphi = 0°$ (c) $\theta = 35°, \varphi = 90°$

(d) $\theta = 35°, \varphi = 180°$ (e) $\theta = 35°, \varphi = 270°$

Fig. 4: Matching of image pairs at different angles of elevation (θ) and azimuth (ϕ).

Each pair of points is then triangulated. The position of each of the points is computed using the user-defined height of the undistortion squares, their orientation, and the width of a pixel, all of which are defined in real world coordinates. We consider the two rays going through these points and the position of their respective imager. These rays should intersect at the physical location of the cloud. However, in practice, they never intersect due to various imprecisions. We thus compute the point which is the closest to both lines, and assume that point to be the location of the cloud. The distance from that point to the light rays gives an estimate of the accuracy of the match and is referred to as triangulation error. A threshold is set to discard wrong feature points matches, whose rays do not converge towards a specific point.

2.3. Grouping

Our aim is to reconstruct clouds rather than individual points. We thus link the reconstructed points if they belong to the same cloud using the following approach.. The matched feature points are first projected on the input fisheye image captured by the first imager. We then compute a Delaunay triangulation, i.e. a triangulation where no point is inside the circumcircle of any triangle [17], the result of which is shown in Fig. 5(a). In order to keep only those triangles which are part of clouds, we perform a cloud/sky segmentation using [18] and keep the triangles with more than half of their surface on cloud regions. This results in the triangles shown in Fig. 5(b). In this way we create separate 3D wire-frame models for each individual cloud.

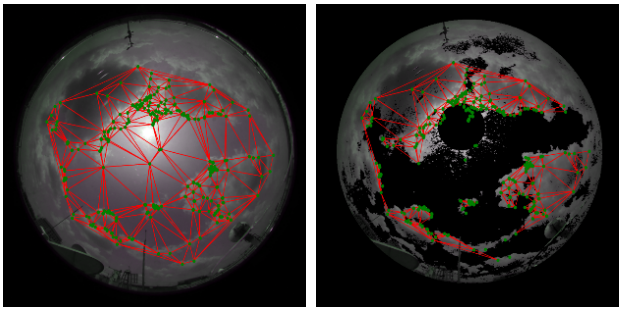

(a) Delaunay triangulation (red) and feature points (green) (b) Segmented input image with filtered triangles

Fig. 5: Construction of wire frames by grouping points belonging to the same cloud.

Figure 7 shows the output of the example used throughout this section. The triangles from Fig. 5(b) are displayed in 3D using the reconstructed locations. The side view demonstrates that the height of each individual cloud is reconstructed separately; the bottom view corresponds well to the input image.

3. VALIDATION

Measuring the altitude of clouds is a complex task, and obtaining reliable ground-truth is challenging; for 3D shape, it is essentially impossible. There exist no standardized and open dataset to compare algorithms, and most of the previous techniques were validated using specialized devices such as ceilometers or lidars.

We benchmark the cloud base reconstruction results from our method with weather radar measurements from Changi weather station, Singapore. We follow the technique of Manandhar et al. [19], providing a high temporal frequency estimate of the occurrence of clouds at any location within the range of the radar. This avoids having to deploy costly devices in close proximity to the imagers. However, the limited scanning elevation angles at which the radar operates provides only a sparse quantization of the altitudes.

Figure 6 shows cloud base height measurements obtained on October 29th, 2015. We see in the top images that the beginning of the day is rather clear with few cumulus clouds,

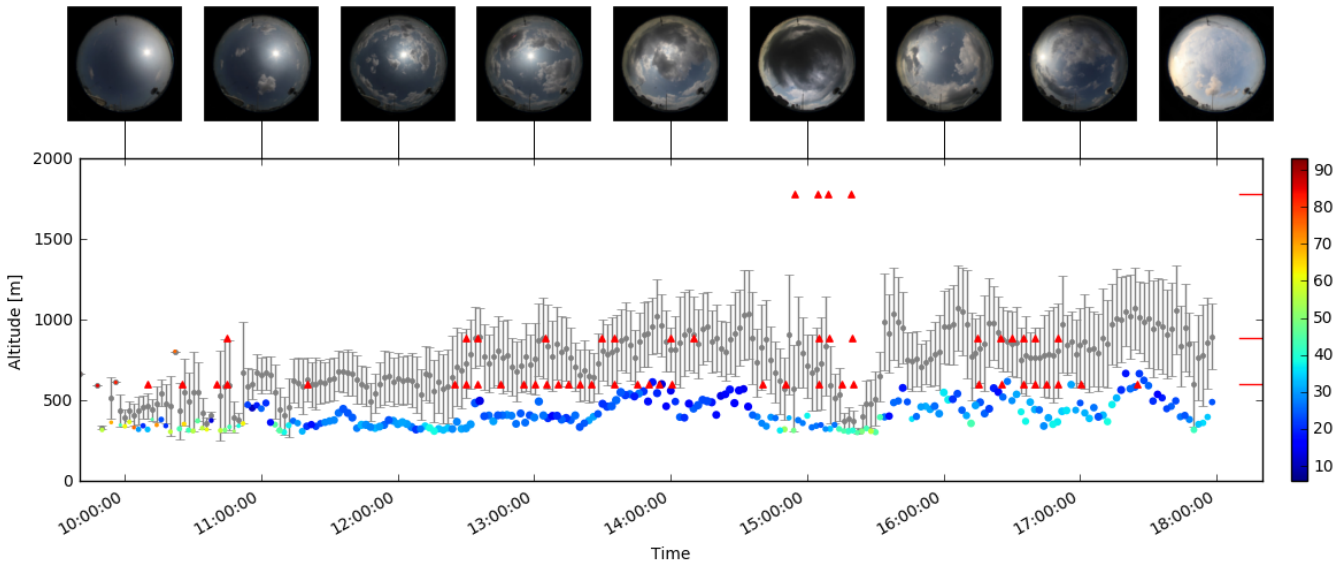

Fig. 6: Cloud base height estimates and their temporal variation from our method compared with data from weather radar. The height distribution of the visual cloud reconstruction at each frame is represented by a dot at the 10th percentile (cloud base height) and by their mean and standard deviation in gray. The dot size is proportional to the number of feature point pairs, while the color reflects the average triangulation error (distance between light rays). Red triangles indicate clouds detected by the radar (at scan altitudes of 600, 890 and 1780 meters). Images captured every hour are shown above the plot.

which are only sparsely detected by the radar due to their low water content. Clouds become denser around 2pm. Around 3pm, a single cloud covers most of the image. Thus, it becomes impossible to reconstruct its height profile, as only the bottom part of the cloud is covering the entire field of view. We notice that the reconstructed volume becomes higher towards the end of the day, as clouds typically become denser and rise through the day due to convection. Overall, we observe that the clouds estimated with our method correlate well with those detected by the weather radar.

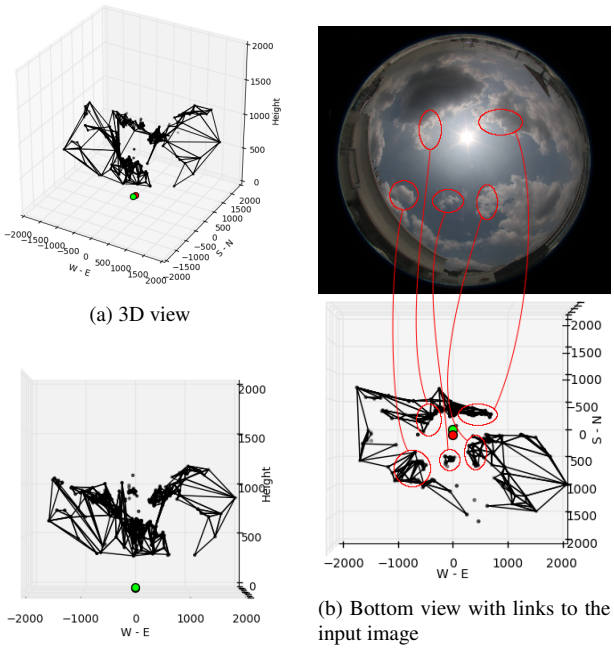

(a) 3D view

(b) Bottom view with links to the input image

(c) Side view

Fig. 7: Result of the 3D wireframe reconstruction. The axes express real world distances in meters, with the origin at the location of the imager represented by the green dot; the other imager is shown as a red dot.

4. CONCLUSION AND FUTURE WORK

In this paper we present a technique to estimate the 3D shape of the cloud base using two ground-based Whole Sky Imagers. We use feature points detection and matching across high-resolution HDR image pairs from both imagers. In combination with sky/cloud segmentation, this allows us to create rough 3D models of the base of individual clouds.

In our future work, we plan to extend this algorithm to more than two imagers with varying distances. We will also use the generated models over several frames for estimation and short-term prediction of cloud movement.

5. REFERENCES

[1] S. Dev, B. Wen, Y. H. Lee, and S. Winkler, "Ground-based image analysis: A tutorial on machine-learning techniques and applications," *IEEE Geoscience and Remote Sensing Magazine*, vol. 4, no. 2, pp. 79–93, June 2016.

[2] S. Dev, F. M. Savoy, Y. H. Lee, and S. Winkler, "Estimation of solar irradiance using ground-based whole sky imagers," in *Proc. IEEE International Geoscience and Remote Sensing Symposium (IGARSS)*, 2016, pp. 7236–7239.

[3] J. X. Yeo, Y. H. Lee, and J. T. Ong, "Performance of site diversity investigated through RADAR derived results," *IEEE Transactions on Antennas and Propagation*, vol. 59, no. 10, pp. 3890–3898, 2011.

[4] S. Dev, F. M. Savoy, Y. H. Lee, and S. Winkler, "WAHRSIS: A low-cost, high-resolution whole sky imager with near-infrared capabilities," in *Proc. IS&T/SPIE Infrared Imaging Systems*. International Society for Optics and Photonics, 2014.

[5] S. Dev, F. M. Savoy, Y. H. Lee, and S. Winkler, "Design of low-cost, compact and weather-proof whole sky imagers for high-dynamic-range captures," in *Proc. IEEE International Geoscience and Remote Sensing Symposium (IGARSS)*, July 2015, pp. 5359–5362.

[6] F. M. Savoy, S. Dev, Y. H. Lee, and S. Winkler, "Geo-referencing and stereo calibration of ground-based Whole Sky Imagers using the sun trajectory," in *Proc. IEEE International Geoscience and Remote Sensing Symposium (IGARSS)*, 2016, pp. 7473–7476.

[7] S. M. Seitz, B. Curless, J. Diebel, D. Scharstein, and R. Szeliski, "A comparison and evaluation of multi-view stereo reconstruction algorithms," in *Proc. Computer Vision and Pattern Recognition (CVPR)*. IEEE, 2006, pp. 519–528.

[8] M. C. Allmen and W. P. Kegelmeyer Jr., "The computation of cloud-base height from paired whole-sky imaging cameras," *Journal of Atmospheric and Oceanic Technology*, vol. 13, no. 1, pp. 97–113, 1996.

[9] J. E. Shields, M. E. Karr, R. W. Johnson, and A. R. Burden, "Day/night whole sky imagers for 24-h cloud and sky assessment: History and overview," *Applied Optics*, vol. 52, no. 8, pp. 1605–1616, 2013.

[10] G. Seiz, E. P. Baltsavias, and A. Gruen, "Cloud mapping from the ground: Use of photogrammetric methods," *Photogrammetric Engineering and Remote Sensing*, vol. 68, no. 9, pp. 941–951, 2002.

[11] E. Kassianov, C. N. Long, and J. Christy, "Cloud-base-height estimation from paired ground-based hemispherical observations," *Journal of Applied Meteorology*, vol. 44, no. 8, pp. 1221–1233, 2005.

[12] F. M. Janeiro, F. Carretas, K. Kandler, P. M. Ramos, and F. Wagner, "Automated cloud base height and wind speed measurement using consumer digital cameras," in *Proc. IMEKO World Congress*, 2012.

[13] F. M. Savoy, J. C. Lemaitre, S. Dev, Y. H. Lee, and S. Winkler, "Cloud base height estimation using high-resolution whole sky imagers," in *Proc. IEEE International Geoscience and Remote Sensing Symposium (IGARSS)*, 2015, pp. 1622–1625.

[14] J. H. Meeus, *Astronomical Algorithms*, Willmann-Bell, 1991.

[15] P. E. Debevec and J. Malik, "Recovering high dynamic range radiance maps from photographs," in *Proc. ACM SIGGRAPH*. ACM, 1997.

[16] D. G. Lowe, "Distinctive image features from scale-invariant keypoints," *International Journal of Computer Vision*, vol. 60, no. 2, pp. 91–110, 2004.

[17] S. Fortune, "Voronoi diagrams and Delaunay triangulations," *Computing in Euclidean Geometry*, vol. 1, pp. 193–233, 1992.

[18] S. Dev, Y. H. Lee, and S. Winkler, "Color-based segmentation of sky/cloud images from ground-based cameras," *IEEE Journal of Selected Topics in Applied Earth Observations and Remote Sensing*, vol. 10, no. 1, pp. 231–242, Jan 2017.

[19] S. Manandhar, F. Yuan, S. Dev, Y. H. Lee, and Y. S. Meng, "Weather radar to detect cloud occurrence level," in *Proc. IEEE Region 10 Conference (TENCON)*, 2016.